# Matrix Mechanics Regulate Engineered Myocardial Microtissue Organization and Contractility

Samuel J. DePalma[1], Austin E. Stis[1], Darcy Huang[1], Javiera J. Vallejos[1], Jason Lo[1], Christopher D. Davidson[1], Aamilah Chowdhury[1], Maggie E. Jewett[1], Adam S. Helms[2], David A. Nordsletten[1,3], Brendon M. Baker[1]

[1]*Department of Biomedical Engineering, University of Michigan, Ann Arbor, MI*
[2]*Division of Cardiovascular Medicine, University of Michigan, Ann Arbor, MI*
[3]*Department Cardiac Surgery, University of Michigan, Ann Arbor, MI*

**Introduction:** The mechanical function of the myocardium is dictated by contractile cardiomyocytes (CMs) and the fibrous extracellular matrix (ECM) that surrounds, organizes, and supports CM bundles [1]. Previous studies have implicated ECM mechanics in driving CM tissue assembly and overall tissue contractile function through mechanosensitive costameres, the cardiomyocyte-ECM adhesion complexes [2-6]. However, due to limitations in existing engineered models of myocardium which require the inclusion of stromal cells and lack orthogonal mechanical control over matrix properties, how CMs sense and respond to specific mechanical microenvironmental changes has not been established. Therefore, improved *in vitro* models of the cardiac ECM are necessary to advance our understanding of how matrix mechanics impact tissue assembly and function. Here, we established a method for creating arrays of cardiac microtissues composed of user-defined synthetic, fibrous ECM and pure induced pluripotent stem cell derived-CMs (iPSC-CMs) that support real-time contractile force readouts. Using this platform, we explored the effects of tissue mechanical inputs, including matrix alignment, matrix stiffness, and boundary mechanics, on engineered cardiac tissue assembly and function. Additionally, we investigated how ECM stiffness impacts iPSC-CM focal adhesion formation, subsequent myofibril development, and the mechanisms underlying CM mechanosensing in physiologically relevant microenvironments.

**Methods:** Arrays of cardiac microtissues were generated by selective photo-crosslinking of electrospun dextran vinyl sulfone (DVS) fiber matrices deposited onto microfabricated PDMS cantilevers (**Fig. 1a**) [7]. Matrix and cantilever stiffnesses were tuned by adjusting photoinitiator concentrations and cantilever height, respectively, while matrix alignment was controlled by altering the translation speed of collection substrates during fiber deposition (**Fig.1d,e**) [7]. PDMS cantilever mechanics were characterized by deflecting individual cantilevers with a tungsten rod of known elastic modulus (**Fig. 1d**). Bending stiffness was calculated by measuring the cantilever deflection and the force applied by the tungsten rod using custom Matlab scripts. Matrix modulus was determined by pressing a microfabricated SU-8 rectangle across the center of the fiber matrices to apply a tension on the matrix (**Fig. 1e**). Using custom Matlab scripts, matrix modulus was extrapolated from measured cantilever deflection. Following mechanical characterization, iPSC-CMs, differentiated and purified via previously described methods [7], were patterned onto matrices using a microfabricated seeding masks cast from 3D-printed molds (**Fig.1a-c**). The contractile stress of microtissues was measured by live-cell time-lapse imaging of PDMS cantilever deflections. Analysis was conducted on d7 after seeding unless otherwise noted and quantified using custom MATLAB scripts. Statistical significance was determined by one-way ANOVA, two-way ANOVA or Student's t-test where appropriate, with significance indicated by $*p < 0.05$. Data is presented as mean + std.

**Results:** Fibrous matrices were fabricated by electrospinning DVS fibers onto an array of microfabricated PDMS posts (98 pairs of posts spaced 448 μm apart) affixed to a rotating mandrel [7] (**Fig. 1a**). Fibers were then selectively crosslinked through a chrome mask and iPSC-CMs were patterned on matrices through a microfabricated seeding mask (**Fig. 1a,b**). Reproducibility of fibroTUG fabrication and seeding protocol was quantified to confirm consistent tissue formation (**Fig. 1c**).

This culture platform affords tunability over the mechanical properties of the synthetic matrix that CMs are seeded upon as well as how these matrices are mechanically constrained. To demonstrate this, we performed mechanical characterization of the PDMS cantilevers and suspended fiber matrices using custom image analysis techniques (**Fig. 1d,e**). Alterations to post dimensions (**Fig 1a**) defined boundary stiffnesses relevant to healthy and diseased cardiac tissue (**Fig. 1f**) [8,9]. Control of DVS matrix modulus

was determined via microindentation and increased with higher photoinitiator concentration within a physiologically relevant range (**Fig. 1g**) [4,6].

After fully characterizing the platform, we examined how iPSC-CMs respond to alterations in boundary stiffness, matrix stiffness and fiber alignment. In tissues contracting against soft cantilevers (0.41 N/m), tissue contractile stress decreased as fiber stiffness increased (**Fig. 2a**). Additionally, we observed an increase in contractile stress on soft (0.68 kPa) and intermediate stiffness matrices (10.1 kPa) composed of aligned matrix fibers as compared to matrices composed of randomly oriented fibers (**Fig.2a**). This effect was mitigated on stiff (17.3 kPa) matrices, potentially indicating that iPSC-CMs reached a contractile limit (**Fig. 2a**). Interestingly, tissues contracting against stiff cantilevers (1.2 N/m) exerted similar contractile stresses independent of matrix alignment (**Fig. 2b**). This may be explained by the enhanced alignment of myofibrils in non-aligned matrices contracting against stiffer posts whereas myofibril alignment is disrupted on non-aligned matrices contracting against soft posts (0.41 N/m) (**Fig. 2c,d**).

Finally, to examine how CMs interpret mechanical changes of the ECM, we assessed costamere formation on matrices of varied mechanics via immunostaining for vinculin, a key costameric protein that is highly sensitive to mechanical forces (**Fig. 2e-g**). Individual costamere size decreased over time, with tissues on stiff matrices having smaller costameres at both time points (**Fig. 2f**). Despite this slight decrease in costamere size at day 7 in soft matrices, vinculin began localizing to z-discs along myofibrils, potentially to enable more uniform stress distribution throughout the tissue (**Fig. 2e,g**). As prior work shows that β-cardiac myosin plays a critical role in sarcomerogenesis [2], we next treated tissues with a blebbistatin, a broad myosin inhibitor, and mavacamten, a small molecule inhibitor specific to β-cardiac myosin, on day 3 post-seeding to examine the role that myosins might play in myofibril maturation after they have completed the initial assembly process on soft matrices (**Fig. 3a-d**). With both treatments, overall vinculin expression and vinculin localization to z-discs is decreased to levels similar to those observed in tissues assembled on stiff matrices (**Fig. 3a-d**).

**Discussion:** In this work, we developed a novel microfabrication strategy to create fibrous cardiac microtissues of pure iPSC-CMs and examined how alterations in ECM biophysical cues affect cardiac tissue assembly and function. This microtissue platform provides a unique ability to orthogonally define boundary mechanics, matrix stiffness, and matrix architecture, enabling precise exploration of the role that the ECM plays in cardiac mechanosensing and contractile function, while also facillitating tissue fractional shortening, which has been shown to be critical for myofibrillar development and maintenance [4,5]. We highlight the importance of this orthogonal control by showing that matrix stiffness, matrix alignment, and tissue constraint have distinct effects on iPSC-CM function and structure. Intriguingly, we find that decreased matrix disorganization does not result in decreased contractile stress or myofibril organization in when iPSC-CMs are former between stiffer posts (**Fig. 2b-d**). Current work is focused on developing computational models of our tissue system to explore how boundary stiffness may impact the cell-scale mechanical anisotropy sensed by the CMs, thus altering tissue assembly and overall function. Further examination of iPSC-CM mechanosensing revealed altered costamere assembly and localization on matrices of different stiffnesses (**Fig. 2e-g, 3a-d**). As robust costamere formation at z-discs is typical in adult cardiac tissue, this phenotype *in vitro* may represent more mature myofibril structures. Previous work established that β-cardiac myosin, not non-muscle myosin, is necessary for proper myofibril assembly upon initial iPSC-CM seeding [2]. Expanding on these results, we show that the maturation of myofibril structures that takes place after this initial assembly process is also dependent on β-cardiac myosin driven tension. Ongoing studies using this platform will focus on implementing molecular force sensors and live-imaging techniques to further assess the impact of tissue mechanics on myofibril maturation and cellular mechanosensing as tissues assemble in both a healthy and disease-mimicking microenvironments.

**References:** [1] Weber+, *J Am Coll Cardiol,* 1989. [2] Chopra+, *Dev Cell,* 2018. [3] Pandey+, *Dev Cell*, 2018. [4] Ribeiro+, *Proc Natl Acad Sci*, 2015. [5] Tsao+, *Nat Commun*, 2021. [6] McCain+, *Proc Natl Acad Sci*, 2012 [7] DePalma+, *Biomater Sci*, 2021. [8] Boudou+, *J Tissue Eng*, 2011. [9] Leonard+, *J Mol Cell Cardiol*, 2018.

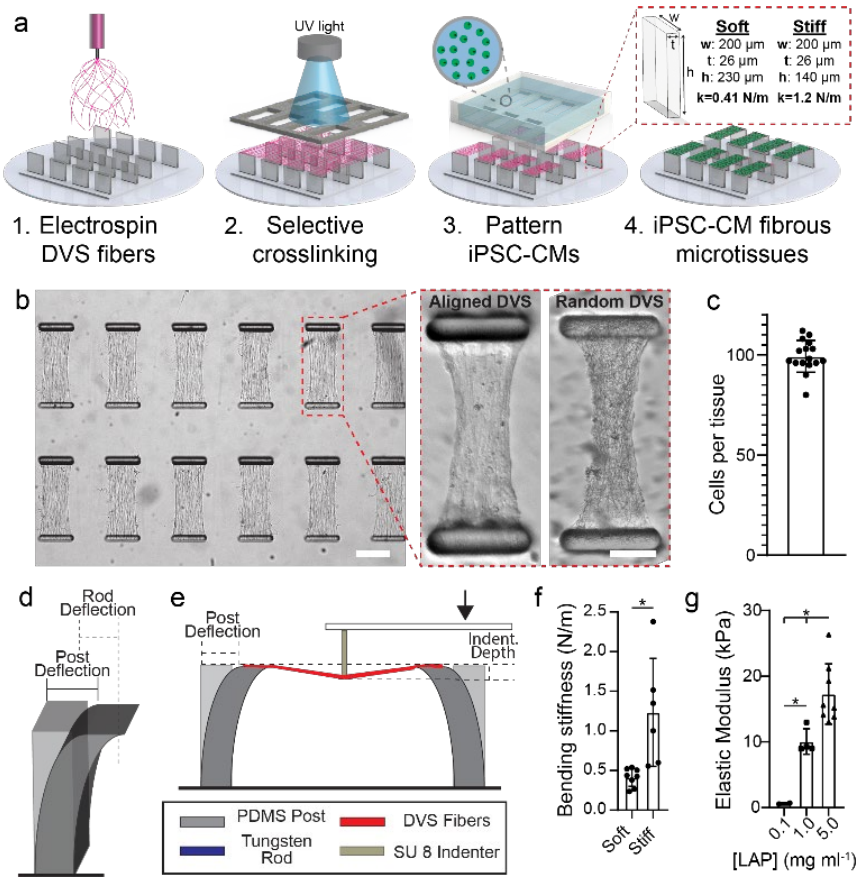


**Figure 1.** a) Cardiac microtissue fabrication scheme. b) Array of suspended matrices (scale bar: 200 µm) and example tissues on aligned and random suspended matrices (scale bar: 100 µm). c) Distribution of CM seeding densities. Schematics of PDMS cantilever (d) and DVS matrix (e) mechanical characterization methods. f) Bending stiffness of soft and stiff cantilevers. g) Elastic modulus of DVS matrices. * indicates statistical significance with $p < 0.05$.

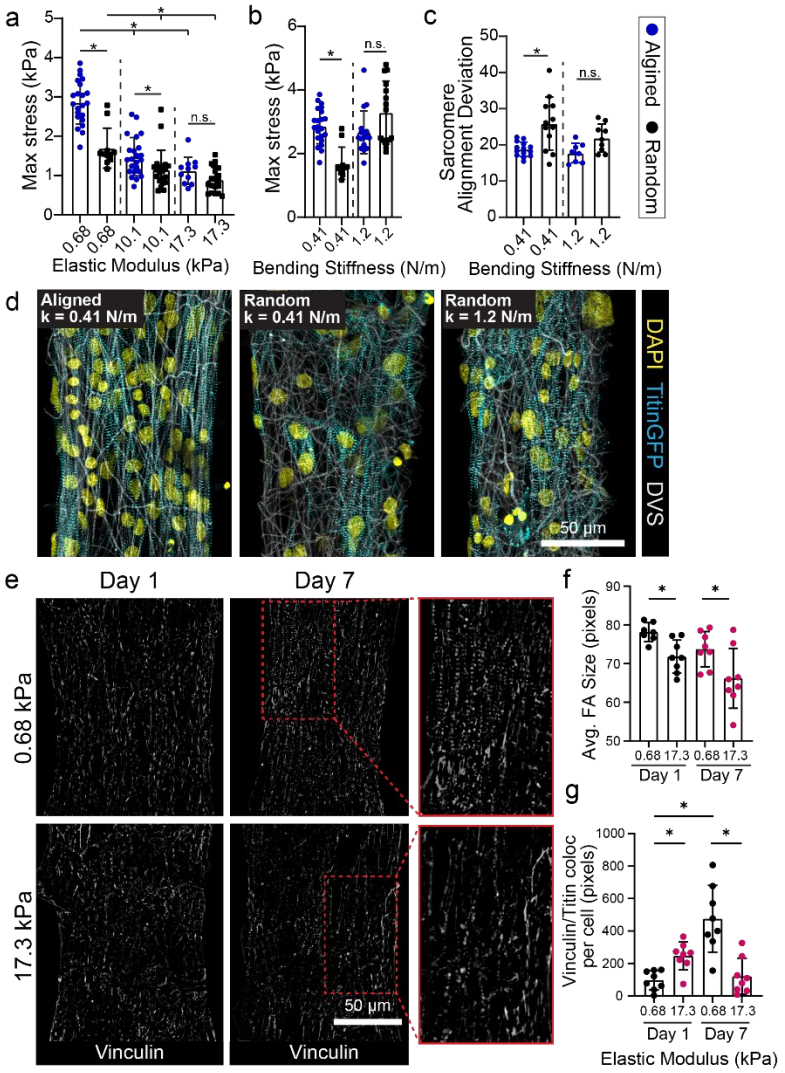


**Figure 2.** Contractile stress of tissues with orthogonal variation of (a) alignment/matrix stiffness and (b) alignment/post stiffness. c) Quantification of sarcomere alignment. d) Confocal fluorescent images of iPSC-CM tissues of varying alignment. e) Confocal fluorescent images of iPSC-CM tissues of varying stiffness at d1 and d7 immunostained for vinculin. Quantification of (f) costamere size and (g) vinculin localization to sarcomere z-discs. * indicates statistical significance with $p < 0.05$.

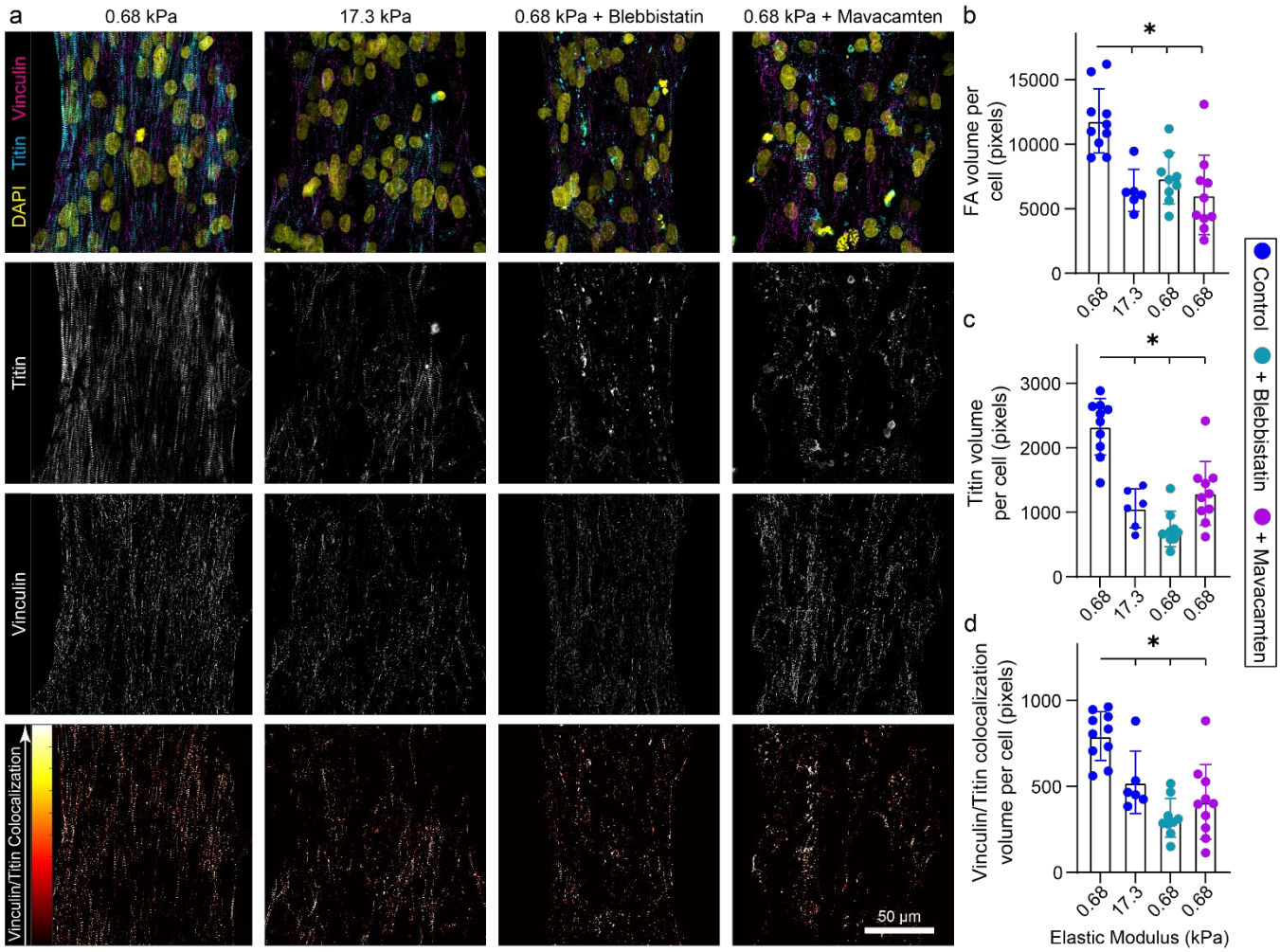


**Figure 3.** a) Confocal fluorescent images of iPSC-CM tissues seeded on matrices of varying stiffness treated with blebbistatin and mavacamten. Heat maps show degree of colocalization between vinculin and titin. Quantification of (b) total costamere formation per cell, (c) overall sarcomere formation via titin fluorescence, and (d) vinculin/titin colocalization. * indicates statistical significance with $p < 0.05$.